

Supplementary Materials: Crop Loss Evaluation Using Digital Surface Models from Unmanned Aerial Vehicles Data

Virginia E. Garcia Millan, Cassidy Rankine and G. Arturo Sanchez-Azofeifa

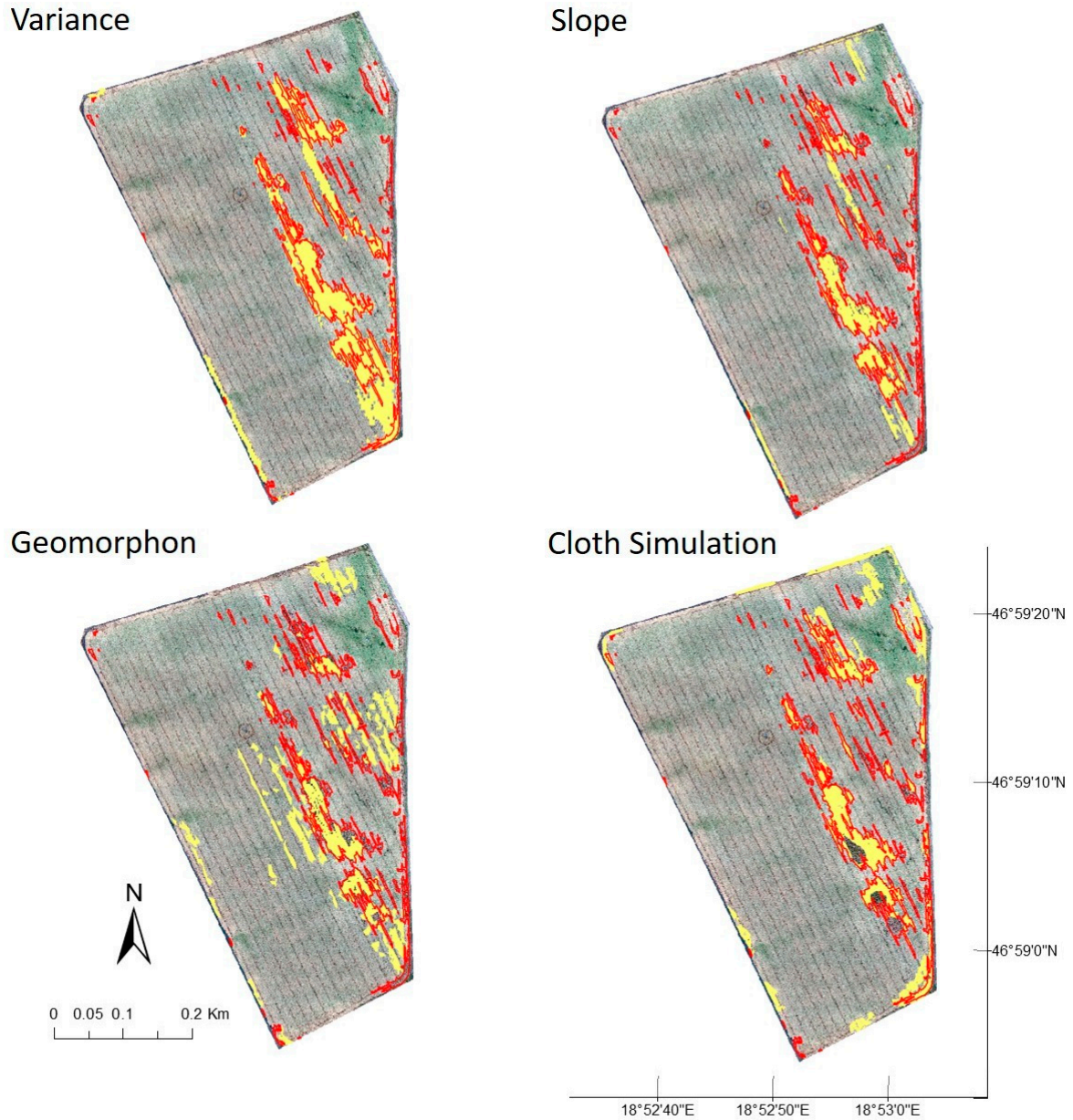


Figure S1. Results of the six terrain analysis and post-processing workflow on dataset W1W (shown in yellow). In red, the damages detected from photointerpretation. UTM WGS84 Zone 34N.

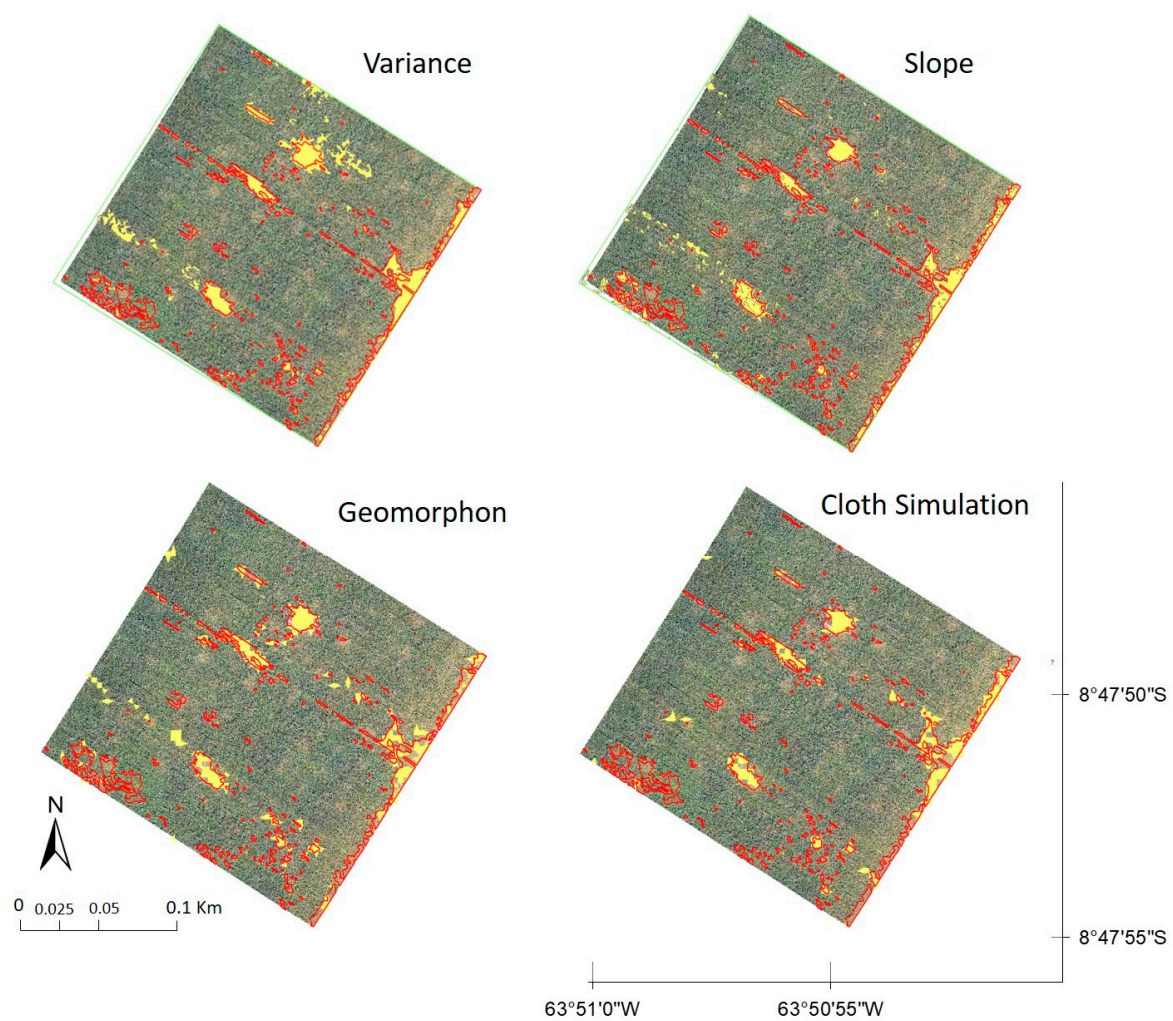
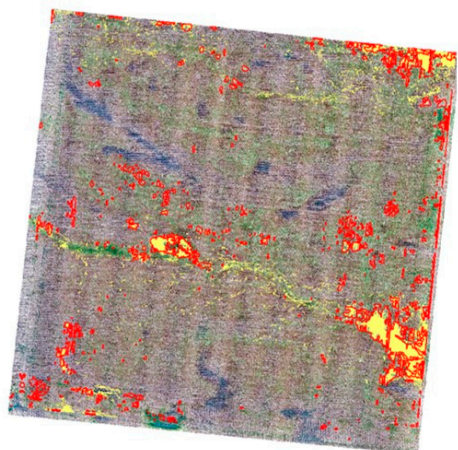
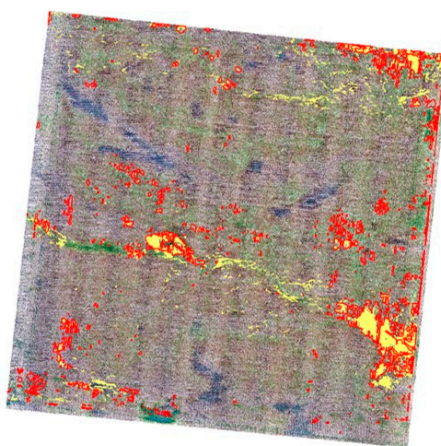


Figure S2. Results of the six terrain analysis and post-processing workflow on dataset C1M (shown in yellow). In red, the damages detected from photointerpretation. UTM WGS84 Zone 20S.

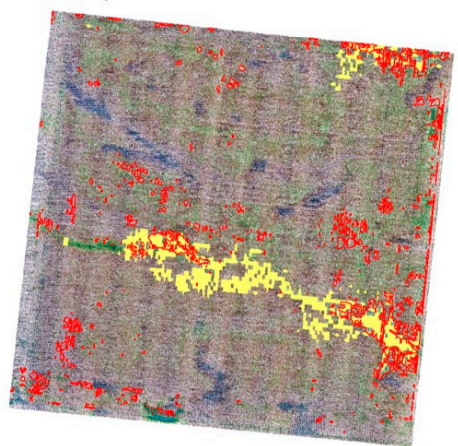
Variance



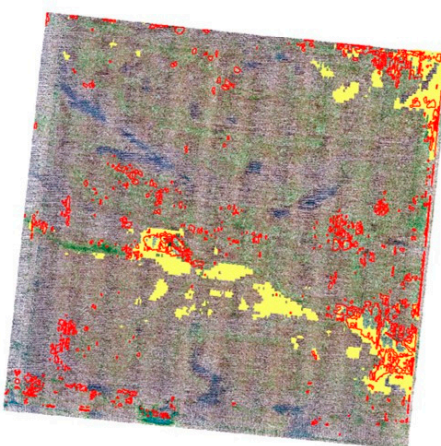
Slope



Geomorphon



Cloth Simulation



0 0.05 0.1 0.2 0.3 Km



106°33'40"W 106°33'20"W 106°33'0"W

52°40'50"N

52°40'40"N

52°40'30"N

Figure S3. Results of the six terrain analysis and post-processing workflow on dataset B1L (shown in yellow). In red, the damages detected from photointerpretation. UTM WGS84 Zone 14N.

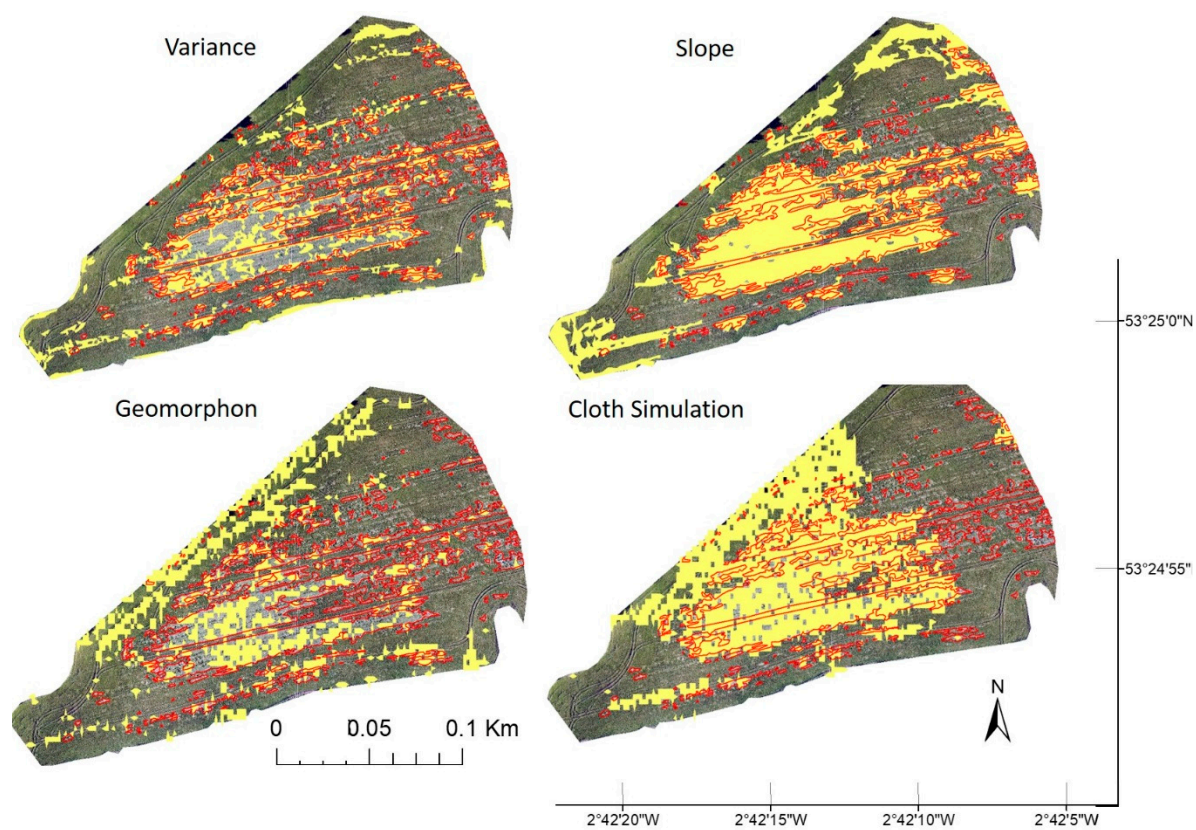


Figure S4. Results of the six terrain analysis and post-processing workflow on dataset W2W (shown in yellow). In red, the damages detected from photointerpretation. UTM WGS84 Zone 30N.

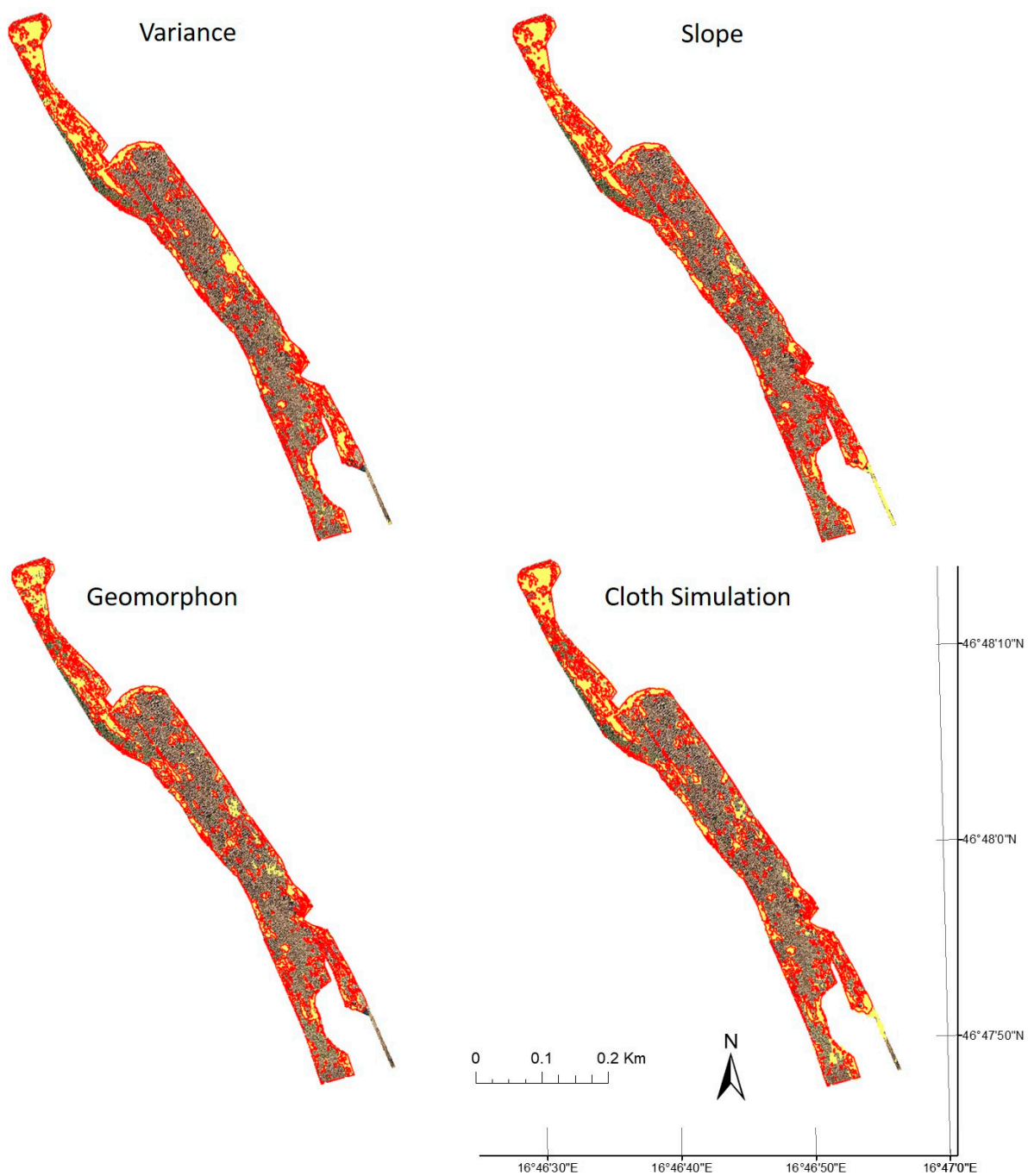


Figure S5. Results of the six terrain analysis and post-processing workflow on dataset C2A (shown in yellow). In red, the damages detected from photointerpretation. UTM WGS84 Zone 33N.

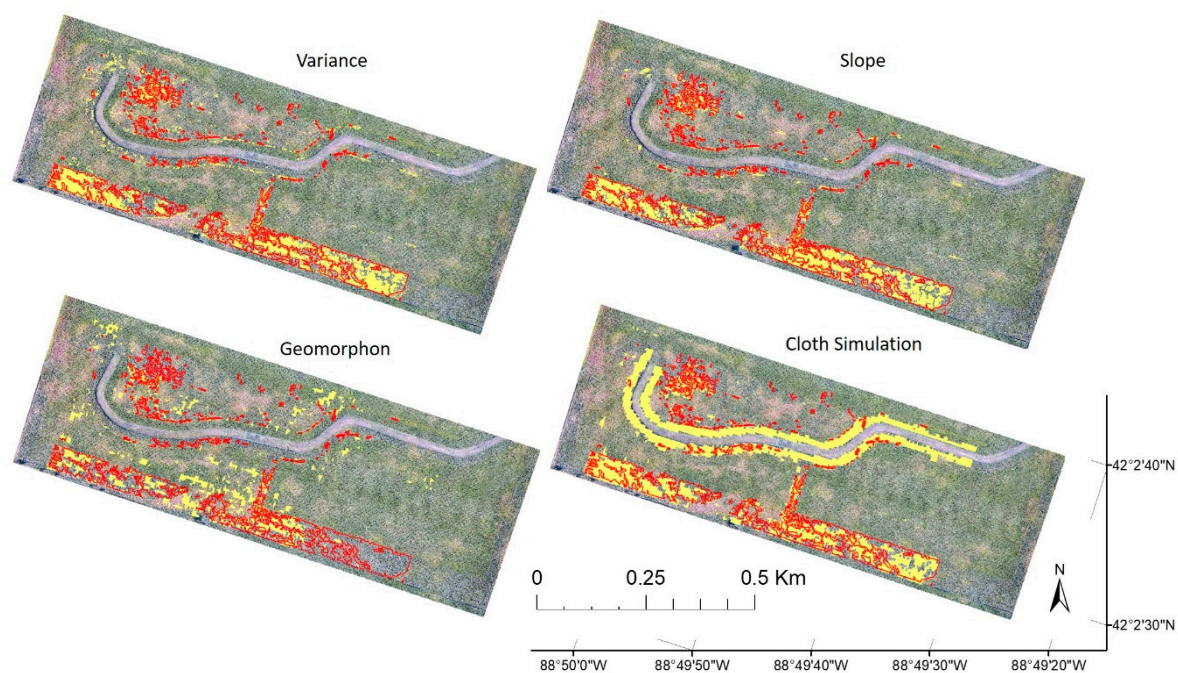


Figure S6. Results of the six terrain analysis and post-processing workflow on dataset C3W (shown in yellow). In red, the damages detected from photointerpretation. UTM WGS84 Zone 16N.